

**Pyrolysis of Napier Grass in a Fixed Bed Reactor : effect of operating conditions on product yields and characteristics**

MOHAMMAD, Isah, ABAKR, Yousif, KABIR, Feroz <<http://orcid.org/0000-0002-3121-9086>>, YUSUF, Suzana, ALSHAREEF, Ibraheem and CHIN, Soh

Available from Sheffield Hallam University Research Archive (SHURA) at:

<http://shura.shu.ac.uk/11743/>

---

This document is the author deposited version. You are advised to consult the publisher's version if you wish to cite from it.

**Published version**

MOHAMMAD, Isah, ABAKR, Yousif, KABIR, Feroz, YUSUF, Suzana, ALSHAREEF, Ibraheem and CHIN, Soh (2015). Pyrolysis of Napier Grass in a Fixed Bed Reactor : effect of operating conditions on product yields and characteristics. *BioResources*, 10 (4), 6457-6478.

---

**Copyright and re-use policy**

See <http://shura.shu.ac.uk/information.html>

# Pyrolysis of Napier Grass in a Fixed Bed Reactor: Effect of Operating Conditions on Product Yields and Characteristics

Isah Yakub Mohammed,<sup>a,\*</sup> Yousif Abdalla Abakr,<sup>a</sup> Feroz Kabir Kazi,<sup>b</sup> Suzana Yusuf,<sup>c</sup> Ibraheem Alshareef,<sup>d</sup> and Soh Aik Chin<sup>d</sup>

This study presents a report on pyrolysis of Napier grass stem in a fixed bed reactor. The effects of nitrogen flow (20 to 60 mL/min), and reaction temperature (450 to 650 °C) were investigated. Increasing the nitrogen flow from 20 to 30 mL/min increased the bio-oil yield and decreased both bio-char and non-condensable gas. 30 mL/min nitrogen flow resulted in optimum bio-oil yield and was used in the subsequent experiments. Reaction temperatures between 450 and 600 °C increased the bio-oil yield, with maximum yield of 32.26 wt% at 600 °C and a decrease in the corresponding bio-char and non-condensable gas. At 650 °C, reductions in the bio-oil and bio-char yields were recorded while the non-condensable gas increased. Water content of the bio-oil decreased with increasing reaction temperature, while density and viscosity increased. The observed pH and higher heating values were between 2.43 to 2.97, and 25.25 to 28.88 MJ/kg, respectively. GC-MS analysis revealed that the oil was made up of highly oxygenated compounds and requires upgrading. The bio-char and non-condensable gas were characterized, and the effect of reaction temperature on the properties was evaluated. Napier grass represents a good source of renewable energy when all pyrolysis products are efficiently utilized.

*Keywords:* Napier grass; Pyrolysis; Bio-oil; Bio-char; Non-condensable; Characterization

*Contact information:* a: Energy, Fuel and Power Technology Research Division, School of Engineering, the University of Nottingham Malaysia Campus, Jalan Broga, 43500 Semenyih, Selangor Darul Ehsan, Malaysia; b: Department of Chemical Engineering and Applied Chemistry, Aston University, Aston Triangle, Birmingham, B4 7ET, United Kingdom; c: Department of Chemical Engineering, Universiti Teknologi Petronas (UTP) Bandar Seri Iskandar, 31750, Tronoh Malaysia; d: Crops for the Future, the University of Nottingham Malaysia Campus, Jalan Broga, 43500 Semenyih, Selangor Darul Ehsan, Malaysia; \*Corresponding author: kebx3iye@nottingham.edu.my

## INTRODUCTION

Fossil fuel is a major source of energy worldwide. The current demand for fossil oil stands at about 94.4 million barrels per day (OMR 2015) and may continue to rise as the population increases. This will definitely put pressure on reserves, estimated at around 1477 billion barrels globally (OPEC 2013), as, under this trend, known oil deposits are expected to be used up in less than 50 years, leading to potential energy crises. This energy insecurity, together with environmental problems associated with fossil fuels, necessitates alternative sources of energy (Anex *et al.* 2010; Leibbrandt *et al.* 2011; Damartzis and Zabaniotou 2011; Saidura *et al.* 2011; Floudas *et al.* 2012; Gebreslassie *et al.* 2013; Liew *et al.* 2014). Solar, wind, geothermal, ocean wave, mini-hydro, and biomass power are renewable energy sources that may help mitigate emission of greenhouse gases (GHGs),

and acid rain pre-cursors in addition to maintaining energy security (Venderbosch and Prins 2010; Park *et al.* 2014; Ming *et al.* 2014). Among the available sources of renewable energy, biomass is the only renewable resource that has carbon in its building blocks which can be processed to liquid fuel.

The use of lignocellulosic biomass (non-food materials) such as forest residues, agro-wastes, energy grasses, aquatic plants, algae *etc.*, for biofuel production continue to gain tremendous attention as they are evenly distributed across the globe. These have also diminished the initial public insecurity associated with first generation biofuels which were produced from food materials (Margeot *et al.* 2009; Nigam and Singh 2011; Srirangan *et al.* 2012). In addition, these materials have low levels of sulfur, nitrogen, and ash, which makes them relatively environmentally friendly. Napier grass (*Pennisetum purpureum*) is one of the perennial grasses with potentials of high biomass yield typically in the range of 25 to 35 oven dry tons per hectare annually which correspond to 100 barrels of oil energy equivalent per hectare compared to other herbaceous plants. Other advantages of Napier grass include compatibility with conventional farming practices, ability to outcompete weeds, and very little or no need for supplementary nutrients, so they therefore have lower establishment costs. It can be harvested up to four times within a year with a ratio of energy output to energy input of around 25:1, which makes it one of the best potential energy crops for development of efficient and economic bioenergy systems (Samson *et al.* 2005). Furthermore, our recent trials in the field have demonstrated that Napier grass can be intercropped with oil palm. The study was conducted under 70% and 50% shade levels with a full sunlight treatment as control. The plant showed more potential for higher dry weights in shaded conditions due to elongated stems, which contained more biomass than the higher leaf biomass in unshaded conditions. This suggests that shaded Napier grass accumulates longer and thicker stems in an attempt to reach better quality light. Intercropping Napier grass with oil palm will offer higher biomass yield, minimize unused spaces in oil palm plantations (estimated at 26.63% of the total plantation area), and bring added economic value to the oil palm industries.

Pyrolysis is a thermochemical process in which materials are converted into solid (bio-char), liquid (bio-oil), and gaseous products (non-condensable) under an inert environment. The product distribution varies depending on how well the process parameters such as nitrogen flow, heating rate, reaction temperature, vapor residence time, and the temperature regime between the reaction and cooling zone are manipulated during the process (Bridgwater 2012). This operational condition has led to the categorization of pyrolysis into slow, intermediate, gasification, and fast pyrolysis processing options. Slow pyrolysis is also referred to as carbonization. It is carried out at temperature up to 400 °C, 60 mins to days, with products distribution of about 35% bio-char, 30% bio-oil, and 35% non-condensable gas. For intermediate pyrolysis, operating conditions are 500 °C and vapor residence time of approximately 10 to 30 s. About 50% of the total product yield is bio-oil, while bio-char and non-condensable gas account for the remaining, which may be in equal proportion. Fast pyrolysis can produce up to 80% bio-oil, 12% bio-char, and 13% non-condensable gas (Bridgwater 2012). Process conditions here involved temperatures around 500 °C, high heating rate, rapid char removal from reaction zone, short vapor residence time of about 1 s, and rapid cooling of volatile. Generally, for optimum bio-oil yield, the temperature between the reaction and cooling zones is expected to be around 400 to 500 °C, and this is meant to prevent any further reaction between the chemical intermediate in the vapor before cooling (Bridgwater 2012; Xiu and Shahbazi 2012; Fernandez-Akarregi *et al.* 2013).

Production of bio-oil from Napier grass *via* pyrolysis has not been studied extensively. Only recently, Strezov *et al.* (2008) have demonstrated the pyrolysis of Napier grass using a computer-aided thermal analyzer, with which the effect of heating rate on the pyrolysis product was investigated. Their findings reveal that a higher heating rate could increase the bio-oil yield with less acidic compounds. Similar observations regarding the bio-oil yield with increasing heating rate were also recorded by Lee *et al.* (2010) in the pyrolysis study of Napier grass in an induction-heating reactor. The bio-oil was found to be acidic and has a high level of oxygenated compounds. Further pyrolysis study of this material, and detailed products characterization, is therefore needed in order to fully understand the effect of process parameters on products distribution and quality for effective, and efficient bioenergy system. The objective of this study was to investigate the effects of process parameters (pyrolysis temperature and nitrogen flow rate) on pyrolysis of Napier grass in a fixed bed reactor, as well as the products distribution.

## EXPERIMENTAL

### Materials, Characterization, and Pyrolysis

Fresh Napier grass stem chopped to 6 to 8 cm was collected from Crops for the Future (CFF) Field Research Centre and was transported in plastic bags to the research building of the University of Nottingham Malaysia campus. The materials were oven dried at 105 °C for moisture content determination according to the BS EN 14774-1 (2009) standard. The dried materials were then shredded in a rotor beater mill Retsch (Germany) to particle sizes of 0.2 to 2 mm and stored in air tight plastic bags for further studies. The volatile matter and ash content on a dry basis were determined according BS EN 15148 (2009) and BS EN 14775 (2009), respectively. The fixed carbon content was computed by subtracting the percentage compositions of ash and volatile matter from the bone dry sample mass. Higher heating value (HHV) was determined using oxygen bomb calorimeter Parr 6100 (USA) following BS EN 14918 (2009). The elemental compositions were determined using CHNS analyzer (LECO Corporation, USA). Biomass ash composition was analyzed by energy dispersive X-ray analysis (Oxford Instruments, UK, X-Max 20 mm<sup>2</sup>). Thermogravimetric study (TGA) was carried out using a Perkin Elmer simultaneous thermal analyzer (STA 6000, USA) in a nitrogen atmosphere, flow rate 20 mL/min at temperature between 300 to 1100 K and heating rate of 10 K/min, and the structural decomposition temperatures were determined. About 10.0 mg (particle size of 0.2 mm) of sample was used. The structural analysis of the biomass was performed according to the procedure outlined in NREL/TP-510-42618 by Sluiter *et al.* (2012).

Pyrolysis was carried out in a fixed bed reactor made from stainless steel (4 cm in diameter, and length 10 cm). The reactor was placed at the center of a stainless steel tubular furnace as shown in Fig. 1. The furnace was heated electrically at the rate of 30 °C/min. The reactor temperature was monitored with a K-type thermocouple connected to a computer through a data logger. 30 g of Napier grass stem (NGS) (0.2 to 2 mm particle size, oven dried) was used in the experiment under nitrogen atmosphere. The reaction time was kept at 15 min ( $\pm 2$  min) after the temperature reached the desired operating temperature or until no significant amount of non-condensable gas was observed. The effect of nitrogen flow rate was first evaluated with 20, 30, 40, 50, and 60 mL/min at a constant reaction temperature of 550 °C ( $\pm 5$  °C). The optimum nitrogen flow was then used in the subsequent pyrolysis where reaction temperatures of 450, 550, 600, and 650 °C were

investigated. The pyrolysis vapor was condensed by passing through a condenser connected to a chiller at 4 °C, and the oil was collected for further analysis. The non-condensable gas was passed through a gas scrubber and the dried gas composition was analyzed. The bio-char was collected at the end of each experiment after the reactor cooled to room temperature, and then was analyzed.

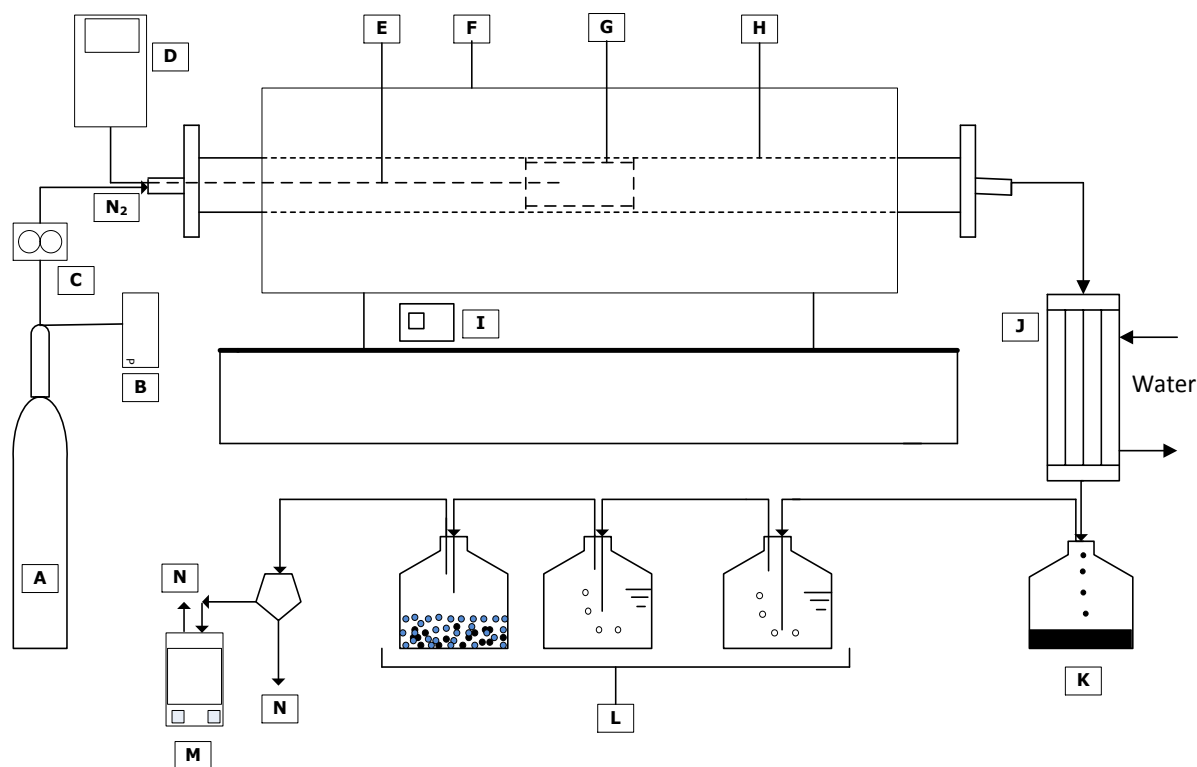


**Fig. 1.** Fixed bed pyrolysis System; (A) nitrogen cylinder; (B) pressure gauge; (C) nitrogen flow meter; (D) data logger connected to PC; (E) K-type thermocouple; (F) tubular furnace; (G) packed bed; (H) alumina tube; (I) furnace control button; (J) condenser connected to chiller with water inflow and outflow; (K) oil collector; (L) gas scrubber; (M) gas analyzer; (N) non-condensable gas discharge

#### *Pyrolysis products characterization*

After each production of bio-oil, characterizations were carried out within 24 h. The oil was first filtered using a PTFE syringe filter of 0.45  $\mu\text{m}$  pore size and 13 mm diameter. Higher heating value was determined using an oxygen bomb calorimeter (Parr 6100) according to ASTM D240-09 (2009) and Mohammed *et al.* (2015). A WalkLAB microcomputer pH meter TI9000 (Trans Instruments, Singapore) was used to determine the pH. Density and viscosity were determined using an Anton Paar density meter (DMA 4500 M, USA) and Brookfield (USA) DV-E viscometer, respectively. The water content in bio-oil was determined using Karl Fischer V20 volumetric titrator (Mettler Toledo, USA) according to ASTM E 203-01 (2001) and Mohammed *et al.* (2015a). Elemental compositions of bio-oil were determined using the procedure outlined above. The chemical composition of bio-oil was determined using a gas chromatograph-mass spectrometer (GC-MS) system (PerkinElmer Clarus<sup>R</sup> SQ 8, USA) with a quadruple detector and PerkinElmer-Elite<sup>TM</sup>-5ms column (30m x 0.25mm x 0.25 $\mu\text{m}$ ). The oven was programmed at an initial temperature of 40 °C, ramp at 5 °C /min to 280 °C and held there for 20 min. The injection

temperature, volume, and split ratio were 250 °C, 1 µL, and 50:1 respectively. Helium was used as carrier gas at a flow rate of 1 mL/min. The bio-oil samples in chloroform (10%, w/v) were prepared and used for the analysis. An MS ion source at 250 °C with 70 eV ionization energy was used. Peaks of the chromatogram were identified by comparing with standard spectra of compounds in the National Institute of Standards and Technology (NIST) library. The non-condensable pyrolysis product was monitored at different temperatures, and the compositions were determined using a gas analyzer (Dräger X-am 5000, Germany). Properties of bio-char from different pyrolysis temperatures were analyzed. Proximate and ultimate analyses were carried out following the same procedures used for the feedstock characterization. X-ray diffraction (XRD) was carried out to examine the crystalline nature of the biochar samples and were compared with those from source biomass using PANalytical X'pertPro (CuK $\alpha$  radiation,  $\lambda=0.1541$  nm; Netherlands) between  $2\theta$  angles of 10 to 60° at 25 mA, 45 kV, step size of 0.025°, and 1.0 s scan rate. The nature of chemical bonds and functional groups were evaluated with Fourier transform infrared spectroscopy (FTIR, PerkinElmer Spectrometer, Spectrum RXI) using the potassium bromide (KBr) method. The KBr disc (13 mm diameter translucent) was made from a homogenized 2 mg sample in 100 mg KBr using a CARVER (USA) press at 5.5 tons for 5 min. Spectra were recorded with Spectrum V5.3.1 software within wave number range of 400 to 4000 cm $^{-1}$  at 32 scans and a resolution of 4 cm $^{-1}$ . Scanning electron microscopy (SEM, FEI Quanta 400 FE-SEM) was used to evaluate the surface and structural characteristics of the bio-char. Specific surface area (BET) and pore properties of the bio-char were determined using ASAP 2020 physisorption analyzer (Micromeritics, USA).

## RESULTS AND DISCUSSION

### Feedstock Characteristics

Napier grass stem (NGS) has high moisture content when harvested. The results of proximate and ultimate (CHNSO) analyses on dry basis are shown in Table 1. The results show that NGS has high volatile matter, high carbon content, and low ash content, which may have contributed to the favorable overall heating value. The high carbon content is not surprising since carbon composition of any biomass is directly linked to its lignin, cellulose, and hemicellulose content. Thermogravimetric analysis showed the thermal decomposition of various structural components of NGS (Fig. 2). In Fig. 2, (a) the peak at 478 K is attributed to the decomposition of extractives, while (b) and (c) corresponded to the decomposition of hemicellulose at temperatures 543 K and cellulose at 600 K respectively. The peak beyond 600 K, (d) indicates the decomposition of lignin. No noticeable peak was observed in this region and consequently, it can be deduced that lignin content of NGS has uniform thermal decomposition. The decomposition temperature values are in good agreement with literature values of 373 to 523 K, 523 to 623 K, 623 to 773 K, and above 773 K for extractives, hemicellulose, cellulose, and lignin correspondingly (Raveendran *et al.* 1996; Reddy *et al.* 2009; Mohammed *et al.* 2015b; Mohammed *et al.* 2015c). Structural analysis revealed that NGS has 12.07% extractives, 38.75% cellulose, 19.76% hemicellulose, and 26.99% lignin.

**Table 1.** Characteristics of Napier Grass Stem (NGS)

| Property                                      | Value         |
|---|---------------|
| <b>Proximate analysis (wt. %)</b>             |               |
| Moisture content <sup>a</sup>                 | 75.3 ± 0.21   |
| Volatile matter <sup>b</sup>                  | 81.50 ± 0.30  |
| Ash content <sup>b</sup>                      | 1.75 ± 0.01   |
| Fixed carbon <sup>c</sup>                     | 16.70 ± 0.09  |
| HHV (MJ/kg)                                   | 18.10 ± 0.10  |
| <b>Ultimate analysis (wt. %) <sup>b</sup></b> |               |
| Carbon (C)                                    | 48.60 ± 0.80  |
| Hydrogen (H)                                  | 6.01 ± 0.14   |
| Nitrogen (N)                                  | 0.99 ± 0.03   |
| Sulfur (S)                                    | 0.32 ± 0.01   |
| Oxygen (O) <sup>c</sup>                       | 44.10 ± 0.66  |
| O/C (atomic ratio)                            | 0.91          |
| H/C (atomic ratio)                            | 0.120         |
| <b>Structural composition (wt. %)</b>         |               |
| Cellulose                                     | 38.8 ± 2.30   |
| Hemicellulose                                 | 19.80 ± 1.68  |
| Lignin  | 27.00 ± 1.29  |
| Extractives                                   | 12.07 ± 0.32  |
| <b>EDX Analysis of ash (wt. %)</b>            |               |
| Sodium (Na)                                   | 0.27 ± 0.006  |
| Magnesium (Mg)                                | 2.34 ± 0.075  |
| Aluminum (Al)                                 | 0.93 ± 0.032  |
| Silicon (Si)                                  | 7.44 ± 0.248  |
| Phosphorus (P)                                | 2.31 ± 0.064  |
| Sulfur (S)                                    | 1.47 ± 0.047  |
| Chlorine (Cl)                                 | 16.10 ± 0.471 |
| Potassium (K)                                 | 64.80 ± 2.228 |
| Calcium (Ca)                                  | 4.34 ± 0.129  |

<sup>a</sup> as received at harvest; <sup>b</sup> dry basis; <sup>c</sup> by difference

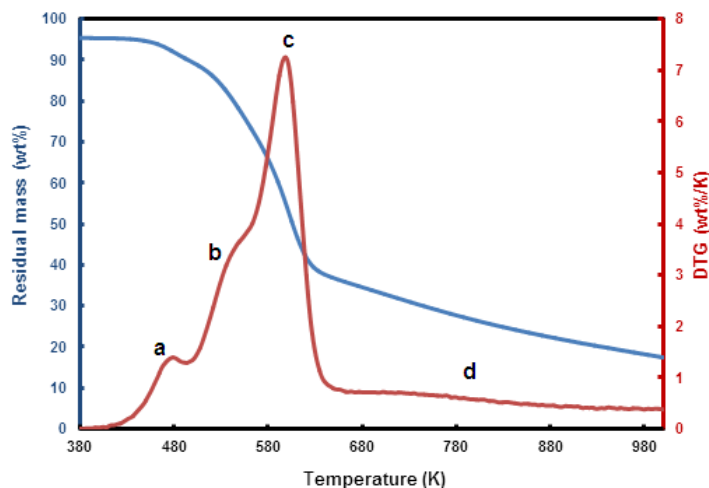


**Fig. 2.** Residual mass ratio and DTG of Napier grass Stem (NGS) on dry basis; (a) extractives; (b) hemicellulose; (c) cellulose; and (d) lignin decompositions, respectively. Conditions: nitrogen atmosphere (20 mL/min); heating rate (10 K/min)

### Effects of Nitrogen Flow Rate and Reaction Temperature on Pyrolysis Products Distribution

Pyrolysis of NGS was first carried out at reaction temperatures of 550 °C and nitrogen flow rate varied between 20 to 60 mL/min. The distribution of pyrolysis products (bio-oil, bio-char, and non-condensable gas) is shown in Fig. 3. The bio-oil yield increased from 27.49% to 31.53% with increasing the nitrogen flow rate from 20 to 30 mL/min. This may be attributed to short pyrolysis vapor residence time in the reaction zone, which minimizes secondary reactions (thermal cracking, repolymerization, and recondensation) that normally favored bio-char formation. Decline in the bio-oil yield was observed with nitrogen flow between 40 to 60 mL/min. This could be as a result of short vapor residence time in the condenser coil which has contributed to yield more non-condensable gas (Uzun *et al.* 2007; Pütün 2010; Keles *et al.* 2011; Soetardji *et al.* 2014).

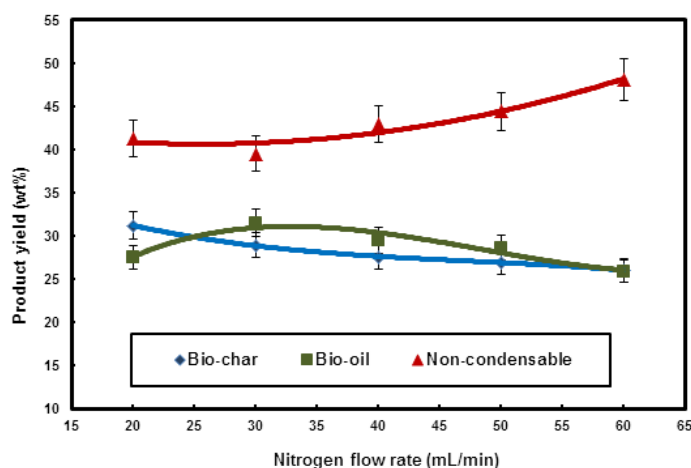


**Fig. 3.** Effect of nitrogen flow rate on pyrolysis products distribution of NGS. Biommas condition: bone dry, 0.2 to 2 mm particle size; heating rate: 30 °C/min; reaction temperature: 550 °C

Generally, an increase in the yield of non-condensable gas was observed with increasing nitrogen flow, while bio-char yield decreased due to the rapid removal of pyrolysis vapor from the reaction zone. In this study, a nitrogen flow of 30 mL/min gave optimum bio-oil yield, and this condition was used in the subsequent experiment.

The effect of reaction temperature on the pyrolysis product distribution was studied at a heating rate of 30 °C /min, and nitrogen flow rate of 30 mL/min. The reaction temperature was varied between 450 to 650 °C. The bio-oil yield was increased with increase of reaction temperature (Fig. 4). At 450 °C, 27.7% oil yield was recorded, which increased to 32.26% at 600 °C. This increase in the oil yield may be as a result of degradation of more lignin, which usually occurs at such a high temperature. Further increase in temperature to 650 °C led to reduction in the oil yield (31.97%), which can be attributed to secondary reactions of pyrolysis vapor at elevated temperature (Jung *et al.* 2008; Imam and Capareda 2012). The yield of non-condensable gas increased with increasing reaction temperature throughout the process. At 450 °C, 26.8% non-condensable was recorded, which increased to 41.47% at 650 °C. This trend, particularly at higher temperature could be due to further cracking of the vapor and more decomposition of bio-char. On the other hand, the bio-char product yield declined with increasing reaction temperature. This is not surprising since the devolatilization of organic materials progresses with increasing temperature. More dehydration of hydroxyl groups and



decomposition of the lignocellulose structure are expected to increase with rise in temperature (Demirbas 2004; Cao and Harris 2010; Muradov *et al.* 2012; Imam and Capareda 2012). Biochar yields of 45.5, 34.69, 29.67, and 26.56% were recorded at 450, 550, 600, and 650 °C, respectively.

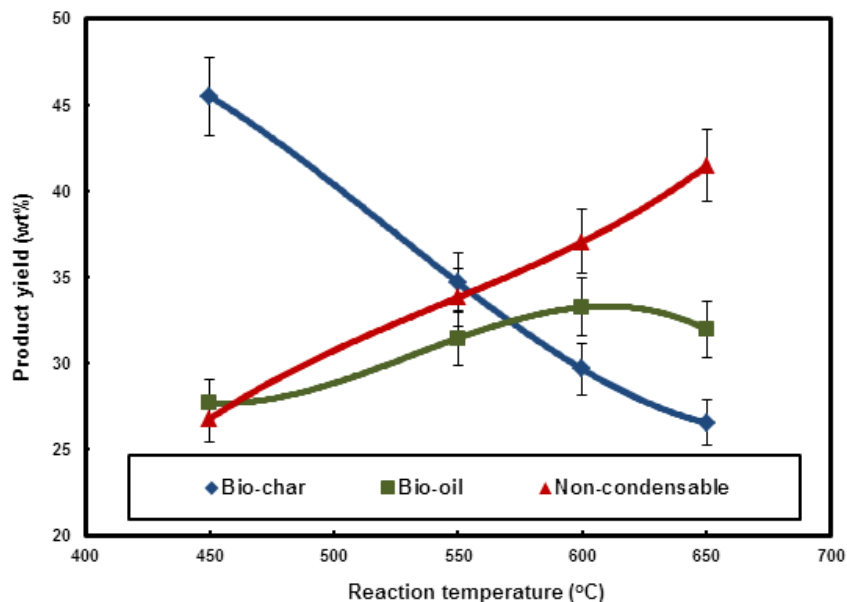


**Fig. 4.** Effect of reaction temperature on pyrolysis products distribution of NGS. Biomass condition: bone dry, 0.2 to 2 mm particle size; heating rate: 30 °C/min, nitrogen flow rate: 30 mL/min.

### Characterization of Bio-Oil, Non-Condensable Gas, and Bio-Char

The physicochemical characteristics and elemental composition of bio-oil obtained are presented in Table 2 according to the reaction temperature. Bio-oil collected at different reaction temperatures in this study appeared as a dark homogenous liquid. Acidity (pH) of the oil was 2.43 to 2.97. This is an indication that the oil may contain a substantial amount of organic acids (AbuBakar and Titiloye 2013; Fan *et al.* 2014). Water content of the oil produced at 450, 550, 600, and 650 °C were 49.42, 47.34, 45.72, and 44.17 wt%, respectively, which were mainly due to the product of dehydration during the pyrolysis reaction (Zhang *et al.* 2007). The decline in moisture content with increasing reaction temperature could be attributed to the extent of cracking of pyrolysis vapor during pyrolysis. Additional thermal cracking during pyrolysis generally yield bio-oil with lower water content and lower molecular weight compounds (Shihadeh and Hochgreb 2002; Zhang *et al.* 2007; Imam and Capareda 2012). The density of the oil increased with decreasing water content, and the values were between 1026 and 1059 kg/m<sup>3</sup>, which are higher than that of gasoline (723 kg/m<sup>3</sup>) and diesel (838 kg/m<sup>3</sup>) fuels. This trend was also true for the viscosity of the oil, which was between 2.45 and 2.79 cp. Similar observations of change in density and viscosity of bio-oil with respect to its water content have been reported by Oasmaa *et al.* (1997), Imam and Capareda (2012), AbuBakar and Titiloye (2013), and Fan *et al.* (2014). Ultimate analysis revealed that the bio-oil had 27.53 to 35.74 wt% carbon, 7.19 to 9.57 wt% hydrogen, 0.83 to 0.85 wt% nitrogen, 0.09 to 0.14 wt% sulfur, and 56.13 to 61.92 wt% oxygen. These changes in the elemental composition are attributed to the reaction temperature during the pyrolysis. Low nitrogen and sulfur contents of the oil suggest that bio-oil from NGS can be used as a source of clean energy.

Higher heating values of the oil were between 25.26 and 28.88 MJ/kg. These values are only about 53 to 61% of the higher heating value of gasoline (47 MJ/kg) and 56 to 62% that of diesel (45 MJ/kg). This is as a result of its higher water and oxygen contents in the oil, and hence there is a need for upgrading.

**Table 2.** Properties of Bio-Oil from Pyrolysis of NGS at Different Reaction Temperatures

| Bio-oil property                     | Reaction temperature (°C) |            |            |            |
|--------------------------------------|---------------------------|------------|------------|------------|
|                                      | 450                       | 550        | 600        | 650        |
| Appearance                           | Dark homogeneous liquid   |            |            |            |
| pH                                   | 2.43±0.01                 | 2.97±0.01  | 2.97±0.01  | 2.82±0.01  |
| Water content (wt%)                  | 49.40±0.24                | 47.30±0.22 | 45.70±0.22 | 44.20±0.21 |
| Density (kg/m <sup>3</sup> ) @ 25 °C | 1030±0.00                 | 1050±0.00  | 1060±0.00  | 1060±0.00  |
| Viscosity (cp) @ 25 °C               | 2.45±0.14                 | 2.67±0.11  | 2.70±0.13  | 2.79±0.14  |
| HHV(MJ/kg)dry basis                  | 25.30±0.10                | 25.40±0.10 | 28.50±0.10 | 28.90±0.10 |
| <b>Elemental composition (wt%)</b>   |                           |            |            |            |
| C                                    | 27.50±0.74                | 30.30±0.84 | 35.20±0.81 | 35.70±0.88 |
| H                                    | 9.57±0.10                 | 7.84±0.14  | 7.27±0.13  | 7.19±0.11  |
| N                                    | 0.84±0.03                 | 0.85±0.03  | 0.83±0.03  | 0.85±0.03  |
| S                                    | 0.14±0.01                 | 0.12±0.01  | 0.10±0.00  | 0.09±0.00  |
| O <sup>*</sup> dry basis             | 24.7±0.66                 | 23.65±0.67 | 22.9±0.58  | 22.1±0.53  |
| H/C(atomic ratio)                    | 0.35                      | 0.26       | 0.21       | 0.20       |
| O/C(atomic ratio)                    | 2.25                      | 2.01       | 1.61       | 1.57       |

\*By difference. Biomass condition: bone dry, 0.2 to 2 mm particle size; heating rate: 30 °C/min; nitrogen flow rate: 30 mL/min.

The chemical composition of bio-oil produced from NGS at 600 °C is presented in Table 3. Twenty seven (27) main chemical compounds were detected by GC-MS. The values quoted below represent the GC-MS peak area (%). The oil contained benzene (12.2%), aliphatic hydrocarbon (1.4%), phenolics (30.5%), furans (18.6%), aldehyde (6.9%), organic acids (10.8%), ketones (2.9%), and esters (10.6%). Some nitrogenous (4.6%) and organic sulfur (0.4%) compounds were also detected. These compounds were further grouped in to hydrocarbons (HC: benzene and aliphatic), value added chemicals (VAC: phenolics, furans, and valuable chemicals), acids, aldehydes and ketones (AAK), esters (E), and sulfur and nitrogenous (NS). The HC represent the main components needed for biofuel, which constitute 13.7% of the bio-oil. They are generally formed during pyrolysis either from the product of partial pyrolysis or volatile compounds from the source biomass (Deshmukh *et al.* 2015). VAC accounted for 50.0%. Phenolics are the product of lignin degradation during the pyrolysis, while furans are the decomposition product of cellulose and hemicellulose (Wang *et al.* 2011; Le Roux *et al.* 2015; Deshmukh *et al.* 2015). These compounds can be further processed to biochemicals and biopolymers that are important feedstocks for the chemical and plastic industries. The presence of AAK in bio-oil has been linked to the decomposition of hemicellulose during pyrolysis (Stephanidis *et al.* 2011; Phan *et al.* 2014). The bio-oil from Napier grass in this study contained 20.7% AAK, which clearly accounts for the low pH value of the oil. This imposes a high requirement on construction materials for storage, transportation, and processing facilities. In addition, AAK compounds are generally responsible for the chemical instability of bio-oil (Zhang *et al.* 2007) in addition to reducing the higher heating

value due to the presence of oxygen in their structure. E compounds are commonly detected in bio-oil as a product of side reaction during pyrolysis. They are formed as a result of esterification acids with primary and second alcohols (Gaertner *et al.* 2010). The amount of E compounds in the bio-oil obtained in this study was 10.6%. These compounds, together with AAK in the oil, are seen to be responsible for the lower value of HHV of bio-oil (Fan *et al.* 2014). The NS detected in the bio-oil can be attributed to nitrogen and sulfur content in the parent biomass. During pyrolysis, the amino acids of the source biomass undergo degradation, which results in the formation of nitrogenous compound in the oil (Deshmukh *et al.* 2015).

The chemical composition of bio-oil from NGS in this study is similar to those obtained by Strezov *et al.* (2008) and Lee *et al.* (2010) from their separate studies on pyrolysis of Napier grass. However, the percentage peak area for the nitrogenous compounds in their bio-oil was higher. This difference may be attributed to the nature of environment in which the Napier grass was grown, and the part of the plant (stems, leaves or stems and leaves) used as feedstock in pyrolysis. In order to improve quality of the bio-oil from NGS to meet the fuel standard, upgrading is necessary, and this will be carried out in future research.

**Table 3.** Chemical Compounds Detected in NGS Bio-Oil Produced at 600 °C and 30 mL/min Nitrogen Flow Rate

| S/No | Compound Name   | Formula   | Retention time (min) | %Area (peak) |
|------|---|---|----------------------|--------------|
| 1    | Benzene   | C <sub>6</sub> H <sub>6</sub>                                 | 2.26                 | 12.2         |
| 2    | Propanoic acid  | C <sub>3</sub> H <sub>6</sub> O <sub>2</sub>                  | 2.87                 | 5.4          |
| 3    | Butanoic acid, 2-methylpropyl ester                             | C <sub>8</sub> H <sub>16</sub> O <sub>2</sub>                 | 3.76                 | 2.1          |
| 4    | Aziridine, 1-methyl   | C <sub>3</sub> H <sub>7</sub> N                               | 4.19                 | 2.8          |
| 5    | Tert-butyl methylcarbonate                                      | C <sub>6</sub> H <sub>12</sub> O <sub>3</sub>                 | 4.37                 | 1.0          |
| 6    | Acetic acid, 2-ethylbutyl ester                                 | C <sub>8</sub> H <sub>16</sub> O <sub>2</sub>                 | 4.81                 | 4.4          |
| 7    | 2-[2-methyl-2-aminoethyl]benzofuran                             | C <sub>11</sub> H <sub>13</sub> NO                            | 5.37                 | 1.6          |
| 8    | Cyclopentane  | C <sub>5</sub> H <sub>10</sub>                                | 5.62                 | 0.9          |
| 9    | Furfural  | C <sub>5</sub> H <sub>4</sub> O <sub>2</sub>                  | 6.04                 | 16.6         |
| 10   | Betazole  | C <sub>5</sub> H <sub>9</sub> N <sub>3</sub>                  | 6.16                 | 1.0          |
| 11   | Cyclohexanemethyl propanoate                                    | C <sub>10</sub> H <sub>18</sub> O <sub>2</sub>                | 8.69                 | 2.7          |
| 12   | Ethanone, 1-(2-furanyl)   | C <sub>6</sub> H <sub>6</sub> O <sub>2</sub>                  | 8.72                 | 2.1          |
| 13   | 3-Hexyne, 2-methyl  | C <sub>7</sub> H <sub>12</sub>                                | 10.86                | 0.6          |
| 14   | Phenol  | C <sub>6</sub> H <sub>6</sub> O                               | 11.2                 | 23.5         |
| 15   | Benzoic acid, 2,3-dihydroxy-6-(2-phenylethyl)                   | C <sub>15</sub> H <sub>14</sub> O <sub>4</sub>                | 14.28                | 5.4          |
| 16   | Benzaldehyde, 4-(octyloxy)-                                     | C <sub>15</sub> H <sub>22</sub> O <sub>2</sub>                | 17.98                | 6.9          |
| 17   | Catechol  | C <sub>6</sub> H <sub>6</sub> O <sub>2</sub>                  | 18.02                | 1.0          |
| 18   | Resorcinol  | C <sub>6</sub> H <sub>6</sub> O <sub>2</sub>                  | 18.06                | 2.6          |
| 19   | Methyl acrylonitrile  | C <sub>4</sub> H <sub>5</sub> N                               | 20.71                | 0.9          |
| 20   | 4H-1-benzopyran-4-one,<br>3-(3,4-dimethoxyphenyl)-6,7-dimethoxy | C <sub>19</sub> H <sub>18</sub> O <sub>6</sub>                | 21.4                 | 0.3          |
| 21   | Methyl tetradec-5-ynoate  | C <sub>15</sub> H <sub>26</sub> O <sub>2</sub>                | 21.91                | 0.4          |
| 22   | Phenol, 2,6-dimethoxy   | C <sub>8</sub> H <sub>10</sub> O <sub>3</sub>                 | 22.12                | 3.3          |
| 23   | 4-Hydroxyphenylacetylketone                                     | C <sub>9</sub> H <sub>8</sub> O <sub>3</sub>                  | 22.65                | 0.5          |
| 24   | Dimethyl tetrathioxalate  | C <sub>4</sub> H <sub>6</sub> S <sub>4</sub>                  | 22.91                | 0.4          |
| 25   | Acethydrazide, N 2-(2-ethoxyphenyl)-                            | C <sub>10</sub> H <sub>14</sub> N <sub>2</sub> O <sub>2</sub> | 23.42                | 0.3          |
| 26   | Benzonitrile, 2-chloro-6-nitro                                  | C <sub>7</sub> H <sub>3</sub> ClN <sub>2</sub> O <sub>2</sub> | 24.49                | 0.5          |
| 27   | 2-methyl-5-(fur-3-yl)-pent-1-en-3-ol                            | C <sub>10</sub> H <sub>14</sub> O <sub>2</sub>                | 25.05                | 0.4          |

The non-condensable gas measured using Dräger X-am 5000 gas analyzer were methane (CH<sub>4</sub>), hydrogen (H<sub>2</sub>), carbon monoxide (CO), and traces of hydrogen sulfide (H<sub>2</sub>S). The presence of H<sub>2</sub>S may be attributed to sulfur in the source biomass. At reaction temperature of 450 °C, CH<sub>4</sub> was not detected and the gas mainly comprises of 0.1075 vol% H<sub>2</sub> and 0.0010 vol% CO (Table 4). The zero value of CH<sub>4</sub> and lower value of CO in the gas are not surprising since they are normally produced from the cracking of volatiles at high temperature (Amutio *et al.* 2012). With increasing temperature, H<sub>2</sub> and CO increased, which went beyond the measuring range (0.2 vol %) of the gas analyzer at 550 °C for H<sub>2</sub> and 600 °C for CO while rapid increase in CH<sub>4</sub> was also observed between 550 and 650 °C. High content of H<sub>2</sub> in the non-condensable gas signifies that it can be used as a source of hydrogen for upgrading of bio-oil to meet the fuel standard. In addition, it can also be processed to transportation fuel via Fisher-Tropsch (FT) synthesis due to the high value H<sub>2</sub>/CO (vol/vol) present (Fernández and Menéndez 2011; Jahirul *et al.* 2012). Although, FT catalysts are very sensitive to H<sub>2</sub>S. They easily get deactivated even at low H<sub>2</sub>S concentration in the feed gas stream (Yamamoto *et al.* 2015). However, this challenge can be addressed during gas cleaning stage prior to FT process through absorption technique with selexol solvent which is relatively cheap (Mohammed *et al.* 2014).

**Table 4.** Composition of Non-Condensable Gas (Nitrogen Free Basis) from NGS Measured using Dräger Xam-5000 Gas Analyzer

| Temperature (°C) | CH <sub>4</sub> (vol %) | H <sub>2</sub> | H <sub>2</sub> S | CO     |
|------------------|-------------------------|----------------|------------------|--------|
| 450              | 0.000                   | 0.107          | 0.001            | 0.001  |
| 550              | 0.530                   | 0.200*         | 0.002            | 0.097  |
| 600              | 2.110                   | 0.200*         | 0.002            | 0.200* |
| 650              | 2.680                   | 0.200*         | 0.004            | 0.200* |

Biomass condition: bone dry, 0.2 to 2mm particle size; heating rate: 30 °C/min; nitrogen flow rate: 30 mL/min. \*Values above maximum detection limit (0.200vol%) of the device

The characteristics of the bio-char from pyrolysis of NGS at various temperatures are given in Table 5. From the proximate analysis, ash content increased slightly with increasing pyrolysis temperature. 12.29% ash content was recorded in the bio-char sample obtained at 450 °C, which increased to 12.56% in the sample pyrolyzed at 650 °C, while volatile matter and higher heating values declined from 26.99 to 21.27% and 29.67 to 27.12 MJ/kg, respectively. The reduction in the volatile content is as a result of removal of more volatiles as the temperature increases during the pyrolysis. This is also responsible for the decrease in the HHV in addition to the increase in the ash content. On the other hand, fixed carbon increased from 60.72% to 65.75% in the bio-char, which indicated that carbonization of bio-char increases with increasing pyrolysis temperature. Ultimate analysis also revealed that the bio-char is predominantly made up of carbon, which increased from 77.37% to 86.05% in the samples produced at 450 °C and 650 °C respectively. Hydrogen and oxygen content were found to decrease with increasing pyrolysis temperature. This may be due to the cleavage and cracking of weak bonds within the bio-char structure (Demirbas 2004; Imam and Capareda 2012; Al-Wabel *et al.* 2013).

Composition of nitrogen in the bio-char sample decreased with increasing pyrolysis. This suggests that some nitrogen containing compounds are released during pyrolysis, which is evident by the presence of nitrogenous compounds in the bio-oil. Comparable observations have been reported by Imam and Capareda (2012) and Song and Guo (2012). Decrease in the sulfur content with increasing pyrolysis temperature may equally be attributed to volatilization of sulfur during pyrolysis (Al-Wabel *et al.* 2013). This was confirmed in this study by the presence of sulfur in the bio-oil (Table 3), and traces of hydrogen sulfide detected in the non-condensable gas (Table 4) which increased with pyrolysis temperature.

**Table 5.** Properties of Bio-Char from NGS Produced at Different Reaction Temperatures on Dry Basis

| Bio-char property                    | Reaction temperature (°C) |            |            |             |
|--------------------------------------|---------------------------|------------|------------|-------------|
|                                      | 450                       | 550        | 600        | 650         |
| <b>Proximate analysis (wt%)</b>      |                           |            |            |             |
| Ash content                          | 12.30±0.24                | 12.50±0.23 | 12.60±0.24 | 12.60±0.24  |
| Volatile matter                      | 27.00±0.19                | 25.80±0.22 | 21.90±0.21 | 21.70±0.20  |
| Fixed carbon <sup>a</sup>            | 60.70±0.44                | 61.70±0.46 | 65.60±0.44 | 65.70±0.44  |
| HHV(MJ/kg)                           | 29.70±0.10                | 27.40±0.10 | 27.60±0.10 | 27.10±0.10  |
| <b>Ultimate analysis (wt%)</b>       |                           |            |            |             |
| Carbon                               | 77.40±0.94                | 80.70±0.92 | 83.90±0.94 | 86.100±0.95 |
| Hydrogen                             | 5.01±0.12                 | 4.31±0.10  | 2.72±0.10  | 1.88±0.09   |
| Nitrogen                             | 1.21±0.03                 | 1.14±0.03  | 1.01±0.03  | 0.73±0.03   |
| Sulfur                               | 0.29±0.01                 | 0.22±0.01  | 0.14±0.01  | 0.10±0.01   |
| Oxygen <sup>a</sup>                  | 16.10±0.20                | 13.60±0.20 | 12.30±0.20 | 11.20±0.19  |
| H/C (atomic ratio)                   | 0.06                      | 0.05       | 0.03       | 0.02        |
| O/C (atomic ratio)                   | 0.21                      | 0.17       | 0.15       | 0.13        |
| <b>Physisorption analysis</b>        |                           |            |            |             |
| BET surface area (m <sup>2</sup> /g) | 0.010±0.00                | 0.060±0.00 | 0.070±0.00 | 0.120±0.00  |
| Pore volume (cm <sup>3</sup> /g)     | 0.002±0.00                | 0.003±0.00 | 0.060±0.00 | 0.076±0.00  |

<sup>a</sup> By difference. Biommas condition: bone dry, 0.2 to 2mm particle size; heating rate: 30 °C/min; nitrogen flow rate: 30 mL/min.

The FTIR spectra of the bio-char produced at different temperatures are compared with that of the original NGS biomass in Fig. 5. The peaks at 3760 and 2927 cm<sup>-1</sup> were assigned to different hydroxyl groups and aliphatic saturated C-H stretching vibration (asymmetric and symmetric methyl and methylene stretching groups) mainly from cellulose content in the biomass sample (Yang *et al.* 2007; Lupoi *et al.* 2014). These peaks disappeared completely in the all bio-char samples, which confirms the decomposition of cellulose in the NGS. Also, the peak around 3400 cm<sup>-1</sup> broadened and decreased in intensity with increasing pyrolysis temperature, indicating the loss of the O-H group due to ignition (Yuan *et al.* 2011; Al-Wabel *et al.* 2013; Mimmo *et al.* 2014). Vibrations around 1600 cm<sup>-1</sup> were due to ring-conjugated C=C bonding in the lignin component of the biomass, which became more pronounced in the bio-char samples with increasing pyrolysis temperature due to newly aromatized and carbonized material from carbohydrate ring dehydration and cyclisation (Pilon and Lavoie 2011; Chia *et al.* 2012). In addition, the disappearance of peak at 1252 cm<sup>-1</sup> due to C-O-C aryl-alkyl ether linkage is an added

indication of increasing aromaticity in the bio-char structure (Al-Wabel *et al.* 2013). The peaks in the neighborhood of  $1150\text{ cm}^{-1}$  to  $900\text{ cm}^{-1}$  are also characteristic peaks of aromatics which became sharper and more pronounced in the bio-char samples (Mukome *et al.* 2013). The fingerprint at  $602\text{ cm}^{-1}$  can be ascribed to alkyl halide in the NGS that disappeared in all the bio-char samples, confirming the degradation the alkyl halide during pyrolysis.

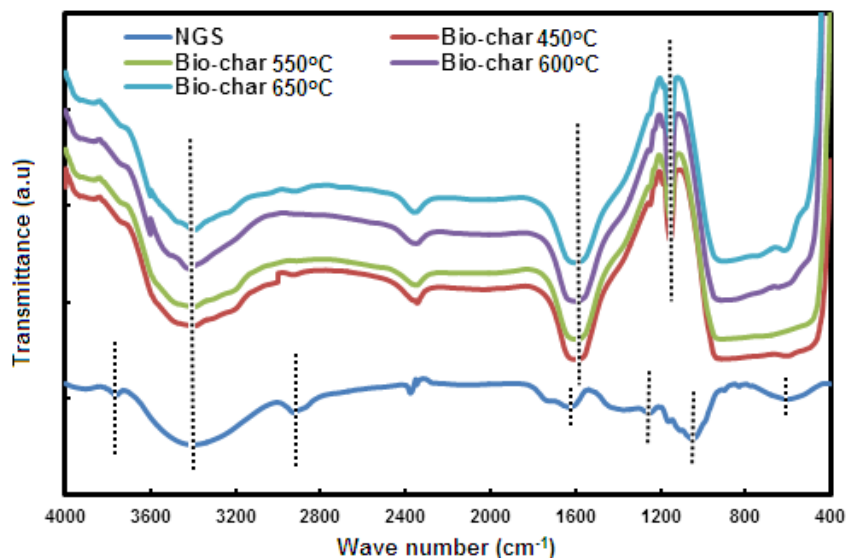


**Fig. 5.** Averaged FTIR spectra (auto-smoothed and auto-baseline corrected) of NGS and bio-char produced at different pyrolysis temperatures

XRD analysis of the bio-char (Fig. 6) shows the disappearance of the cellulose peak ( $2\theta = 22.16^\circ$ ) in the source NGS biomass in all the bio-char. With the increase of pyrolysis temperature, the peak widened and became flat at  $650^\circ\text{C}$ . This observation is in agreement with the FTIR result. New peaks appeared at  $2\theta$  value of  $28.33$ ,  $40.50$ ,  $50.15$ , and  $58.60^\circ$ , which indicate the existence of a crystalline system in the char. XRD search and match revealed that the char samples were predominantly made up of sylvite (KCl) with a crystal system corresponding to those of the new peaks identified (Yuan *et al.* 2011). Sylvite is a good candidate for fertilizer production, and therefore bio-char can be used either as a fertilizer or source of fertilizer. Traces of various barium cerates ( $\text{BaCeO}_3$ ) were also found. This material is an important ingredient in the development of fuel cells (Ketzial *et al.* 2013; Medvedev *et al.* 2014). Further investigation is needed in order to utilize bio-char as an alternative source of barium cerate in fuel cell application. Thermogravimetric analysis (Fig. 7a) revealed that the bio-char had high thermal stability, which increased with pyrolysis temperature (Sun *et al.* 2014). The total weight loss recorded in the sample obtained at  $450^\circ\text{C}$ ,  $550^\circ\text{C}$ ,  $600^\circ\text{C}$ , and  $650^\circ\text{C}$  was 59.43%, 53.02%, 48.45%, and 33.59%, respectively. The DTG results (Fig. 7b) indicated that cellulose, hemicellulose, and lignin components of NGS biomass were completely volatilized, and the weight losses were mainly due to dehydrogenation and aromatization of the bio-char in addition to decomposition of inorganic components (Oja *et al.* 2006; Azargohar *et al.* 2014). The degree of aromaticity in the bio-char structure was evaluated by plotting a Van Krevelen chart, as shown in Fig. 8. The plot showed distinct regions for bio-char, bio-oil, and the source biomass, with bio-char appearing at the lower left hand corner, biomass at the middle, and bio-oil at the top right hand corner. The lower values of H/C and O/C atomic

ratios recorded in the bio-char samples with the increase temperature are indications that an increased degree of aromaticity in the resulting bio-char structure was due to hydration, decarboxylation, and decarbonylation at high temperature, which led to enrichment of the bio-char with carbon, making the surface highly hydrophobic (Chun *et al.* 2004; Kim *et al.* 2011; Ahmad *et al.* 2012; Al-Wabel *et al.* 2013; Azargohar *et al.* 2014; Mimmo *et al.* 2014).

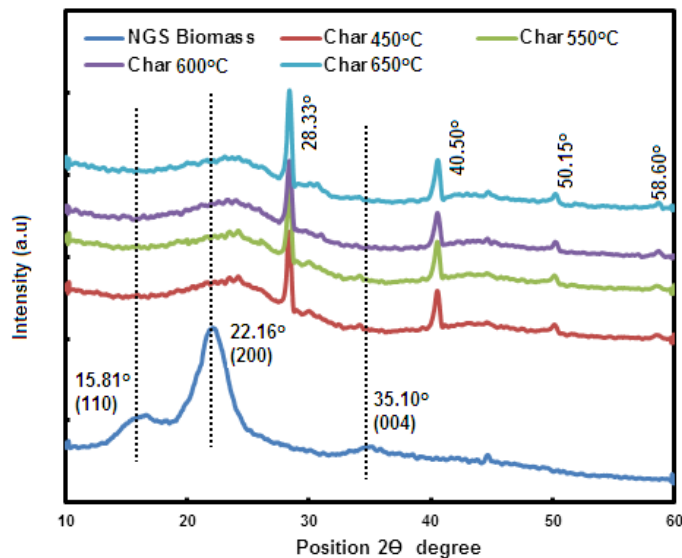
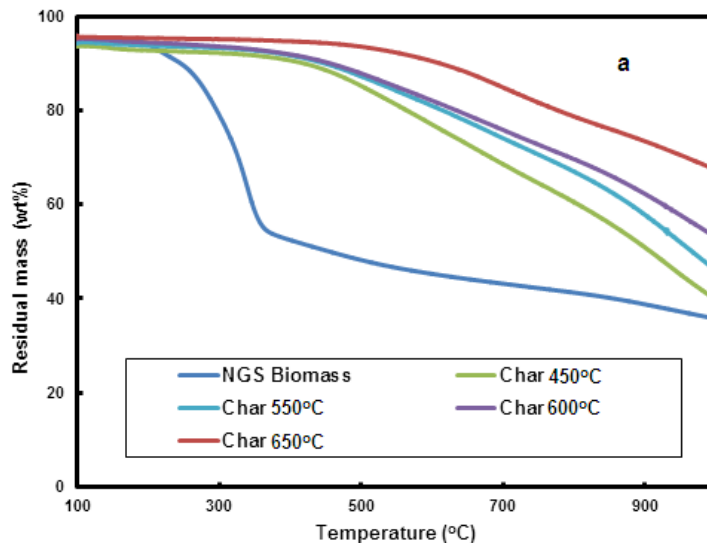
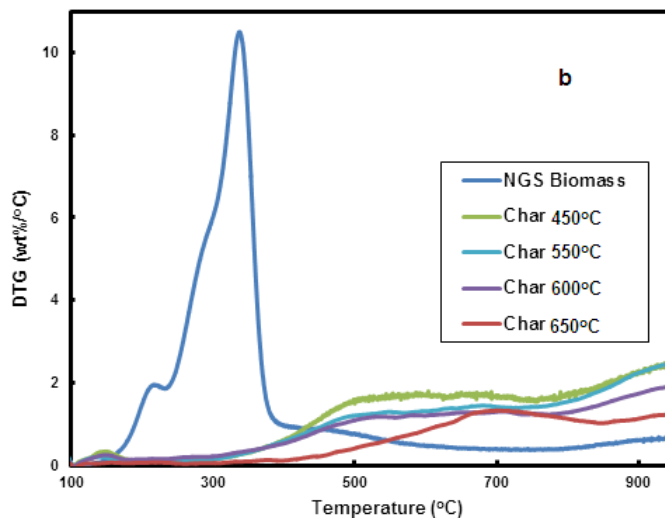
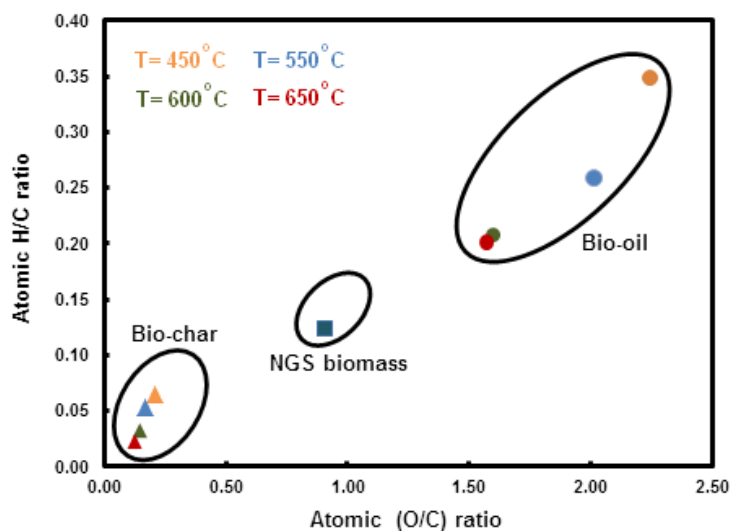


Fig. 6. X-ray diffractogram of NGS and bio-char obtained at different pyrolysis temperature





**Fig. 7.** Thermogravimetric analysis of NGS and bio-char obtained at different pyrolysis temperature. (wt%) residual mass % (a) TG, (b) DTG under nitrogen atmosphere (20 mL/min); heating rate (20 °C/min)



**Fig. 8.** Van Krevelen chart for NGS biomass and bio-char at different pyrolysis temperature

Combustion characteristics and chemical activity of bio-char are largely governed by surface area (Imam and Capareda 2012). This information is needed to further evaluate possible applications of bio-char. Results of SEM analysis carried out on the bio-char samples produced at different pyrolysis temperature are shown in Fig. 9.



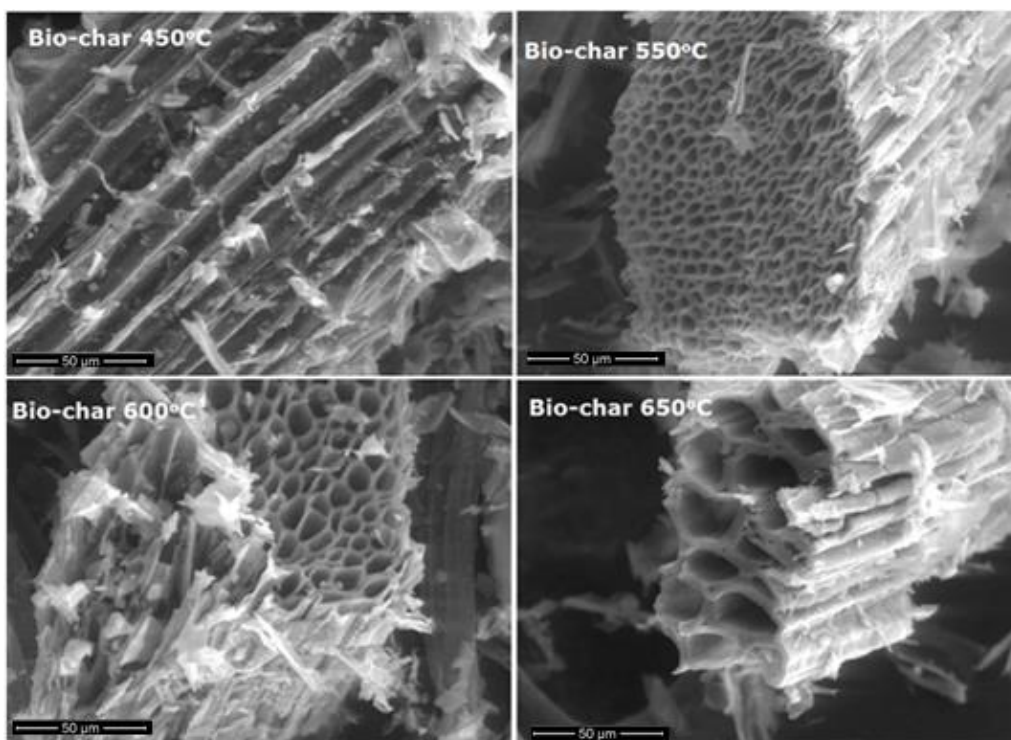


**Fig. 9.** SEM images of NGS bio-char obtained at different pyrolysis temperatures. Scanning conditions: HV (20kV), Mag (1200x), low vacuum

The SEM images show that the bio-chars had cracked and uneven pore structures. The pore sizes tended to increase with increasing pyrolysis temperature, which can be attributed to high degree devolatilization recorded with increasing pyrolysis temperature. The pore structure was further evaluated using a physisorption analyzer, and the results are summarized in Table 5. The specific surface area (BET) of the bio-char was between 0.01 and 0.12m<sup>2</sup>/g with minimum value from sample obtained at 450 °C, while the maximum specific area was recorded correspond to bio-char samples produced at 650 °C. Similar characteristics of bio-char have been reported in the literature (Imam and Capareda, 2012; Wang *et al.* 2013; Abdel-Fattah *et al.* 2015).

## CONCLUSIONS

1. The pyrolysis of Napier grass stem was carried out in a fixed bed. The effects of nitrogen flow and reaction temperature on the pyrolysis products distribution were investigated. Nitrogen flow from 20 to 30 mL/min increased bio-oil yield, while declines in both bio-char and non-condensable gas were recorded. As flow increased from 40 to 60 mL/min, the yields of bio-oil and bio-char decreased, while rapid increase in the non-condensable gas yield was observed. 30 mL/min nitrogen flow gave optimum bio-oil yield and was used in the remaining experiment.
2. Increasing the reaction temperature from 450 °C to 600 °C increased the bio-oil yield, but the yield decreased at 650 °C. The bio-char yield showed continuous decrease with temperature from 450 to 650 °C, while non-condensable gas increased with the rise in

temperature. Bio-oil has properties (low pH, high water, and high oxygen contents) which need upgrading in order to meet the fuel quality standard.

3. Bio-char characteristics revealed that it was porous and highly carbonaceous, properties which increased with reaction temperature. Such biochar may be used as solid biofuel, source of carbon, adsorbent, fertilizer, and for soil aeration. Bio-char may also be useful in the development of fuel cells. Non-condensable gases measured were methane, hydrogen sulfide with high percentages of hydrogen, and carbon monoxide. This may be used as source of hydrogen for upgrading of bio-oil. In addition, it may be processed to liquid fuel *via* the Fischer-Tropsch process. This study has shown that Napier grass is a good source of renewable energy which can be sustained when all the pyrolysis products are efficiently utilized.

## ACKNOWLEDGEMENTS

The project was supported by the Crops for the Future (CFF) and University of Nottingham under the grant BioP1-005.

## REFERENCES CITED

- Abdel-Fattah, T. M., Mahmoud, M. E., Ahmed, S. B., Huff, M. D., Lee, J. W., Kumar, S. (2015). "Biochar from woody biomass for removing metal contaminants and carbon sequestration" *Journal of Industrial and Engineering Chemistry* 22(25), 103-109. DOI:10.1016/j.jiec.2014.06.030
- Abu Bakar, M. S., and Titiloye, J. O. (2013). "Catalytic pyrolysis of rice husk for bio-oil production," *Journal of Analytical and Applied Pyrolysis* 103, 362-368. DOI: 10.1016/j.jaap.2012.09.005
- Ahmad, M., Lee, S. S., Dou, X., Mohan, D., Sung, J. K., Yang, J. E., and Ok, Y. S. (2012). "Effects of pyrolysis temperature on soybean stover- and peanut shell-derived biochar properties and TCE adsorption in water," *Bioresource Technology* 118, 536-544. DOI: 10.1016/j.biortech.2012.05.042
- Al-Wabel, M. I., Al-Omran, A., El-Naggar, A. H., Nadeem, M., and Usman, A. R. A. (2013). "Pyrolysis temperature induced changes in characteristics and chemical composition of biochar produced from conocarpus wastes," *Bioresource Technology* 131, 374-379. DOI: 10.1016/j.biortech.2012.12.165
- Amutio, M., Lopez, G., Artetxe, M., Elordi, G., Olazar, M., and Bilbao, J. (2012). "Influence of temperature on biomass pyrolysis in a conical spouted bed reactor," *Resources, Conservation and Recycling* 59, 23-31. DOI: 10.1016/j.resconrec.2011.04.002
- Anex, R. P., Aden, A., Kazi, F. K., Fortman, J., Swanson, R. M., Wright, M. M., Satrio, J. A., Brown, R. C., Daugaard, D. E., Platon, A., Kothandaraman, G., Hsu, D. D., and Dutta, A. (2010). "Techno-economic comparison of biomass-to-transportation fuels via pyrolysis, gasification, and biochemical pathways" *Fuel* 89, S29-S35. DOI:10.1016/j.fuel.2010.07.015
- ASTM D240 (2009). "Standard test method for heat of combustion of liquid hydrocarbon fuels by bomb calorimeter," *ASTM International*, West Conshohocken, PA.

- DOI:10.1520/D0240-09
- ASTM E203 (2001). "Standard test method for water using volumetric Karl Fischer titration," *ASTM International*, West Conshohocken, PA. DOI:10.1520/E0203-01
- Azargohar, R., Nanda, S., Kozinski, J.A., Dalai, A. K., and Sutarto, R. (2014). "Effects of temperature on the physicochemical characteristics of fast pyrolysis bio-chars derived from Canadian waste biomass," *Fuel* 125, 90-100.  
DOI:10.1016/J.FUEL.2014.01.083
- Bridgwater, A.V. (2012). "Review of fast pyrolysis of biomass and product upgrading," *Biomass and bioenergy* 38, 68-94. DOI:10.1016/J.Biombioe.2011.01.048
- BS EN 14774-1 (2009). "Solid biofuels. Determination of moisture content. Oven dry method. Total moisture," British Standards Institution, London, UK.  
DOI:10.3403/30198050
- BS EN 14775 (2009). "Solid biofuels. Determination of ash content," British Standards Institution, London, UK. DOI:10.3403/30198062
- BS EN 14918 (2009). "Solid biofuels. Determination of calorific value," British Standards Institution, London, UK. DOI:10.3403/30198715
- BS EN 15148 (2009). "Solid biofuels. Determination of the content of volatile matter," British Standards Institution, London, UK. DOI:10.3403/30198059
- Cao, X., and Harris, W. (2010). "Properties of dairy-manure-derived biochar pertinent to its potential use in remediation" *Bioresour. Technol.* 101(14), 5222-5228.  
DOI:10.1016/j.biortech.2010.02.052
- Chia, C. H., Gong, B., Joseph, S. D., Marjo, C. E. Munroe, P., and Rich, A. M. (2012). "Imaging of mineral-enriched biochar by FTIR, Raman and SEM-EDX," *Vibrational Spectroscopy* 62, 248-257. DOI:10.1016/j.vibspec.2012.06.006
- Chun, Y., Sheng, G., Chiou, C.T., and Xing, B. (2004). "Compositions and sorptive properties of crop residue-derived chars" *Environ. Sci. Technol.* 38(17), 4649-4655.  
DOI:10.1021/es035034w
- Damartzis, T., and Zabaniotou, A. (2011). "Thermochemical conversion of biomass to second generation biofuels through integrated process design—A review," *Renewable and Sustainable Energy Reviews* 15(1), 366-378. DOI:10.1016/j.rser.2010.08.003
- Demirbas, A. (2004). "Effects of temperature and particle size on bio-char yield from pyrolysis of agricultural residues," *J. Anal. Appl. Pyrolysis* 72(2), 243-248.  
DOI:10.1016/j.jaap.2004.07.003
- Deshmukh, Y., Yadav, V., Nigam, N., Yadav, A., and Khare, P. (2015). "Quality of bio-oil by pyrolysis of distilled spent of *Cymbopogon flexuosus*," *Journal of Analytical and Applied Pyrolysis*, in press, DOI:10.1016/J.JAAP.2015.07.003
- Fan, Y., Cai, Y., Li, X., Yin, H., Yu, N., Zhang, R., and Zhao, W. (2014). "Rape straw as a source of bio-oil via vacuum pyrolysis: Optimization of bio-oil yield using orthogonal design method and characterization of bio-oil," *Journal of Analytical and Applied Pyrolysis* 106, 63-70. DOI:10.1016/j.jaap.2013.12.011
- Fernández, Y., and Menéndez, J.A. (2011). "Influence of feed characteristics on the microwave-assisted pyrolysis used to produce syngas from biomass wastes," *J. Anal. Appl. Pyrolysis* 91(2), 316-322. DOI:10.1016/j.jaap.2011.03.010
- Fernandez-Akarregi, A.R., Makibar, J., Lopez, G., Amutio, M., and Olazar, M. (2013). "Design and operation of a conical spouted bed reactor pilot plant (25 kg/h) for biomass fast pyrolysis," *Fuel Processing Technology* 112, 48-56.  
DOI:10.1016/j.fuproc.2013.02.022
- Floudas, C. A., Elia, J. A., and Baliban, R. C. (2012). "Hybrid and single feedstock

- energy processes for liquid transportation fuels: A critical review,” *Computers and Chemical Engineering* 41, 24-51. DOI:10.1016/j.compchemeng.2012.02.008
- Gebreslassie, B. H., Slivinsky, M., Wang, B., and You, F. (2013). “Life cycle optimization for sustainable design and operations of hydrocarbon biorefinery via fast pyrolysis, hydrotreating and hydrocracking,” *Computers and Chemical Engineering* 50, 71-91. DOI:10.1016/j.compchemeng.2012.10.013
- Imam, T., and Capareda, S. (2012). “Characterization of bio-oil, syn-gas and bio-char from switchgrass pyrolysis at various temperatures,” *Journal of Analytical and Applied Pyrolysis* 93, 170-177. DOI:10.1016/j.jaap.2011.11.010
- Jahirul, M. I., Rasul, M. G., Chowdhury, A. A., and Ashwath, N. (2012). “Biofuels production through biomass pyrolysis—A technological review,” *Energies* 5(12), 4952-5001. DOI:10.3390/en5124952
- Jung, S.-H., Kang, B.-S., and Kim, J.-S. (2008). “Production of bio-oil from rice straw and bamboo sawdust under various reaction conditions in a fast pyrolysis plant equipped with a fluidized bed and a char separation system,” *Journal of Analytical and Applied Pyrolysis* 82(2), 240-247. DOI:10.1016/j.jaap.2008.04.001
- Keles, S., Kaygusuz, K., and Akgün, M. (2011). “Pyrolysis of woody biomass for sustainable bio-oil,” *Energy Sources Part A* 33, 879-889. DOI:10.1080/15567030903330652
- Ketzial, J., Radhika, D., and Nesaraj, A S. (2013). “Low-temperature preparation and physical characterization of doped BaCeO<sub>3</sub> nanoparticles by chemical precipitation,” *International Journal of Industrial Chemistry* 4(1), 18. DOI:10.1186/2228-5547-4-18
- Kim, P., Johnson, A., Edmunds, C. W., Radosevich, M., Vogt, F., Rials, T. G., and Labbe, N. (2011). “Surface functionality and carbon structures in lignocellulosic-derived bio-chars produced by fast pyrolysis,” *Energy and Fuel* 25(10), 4693-4703. DOI:10.1021/ef200915s
- Le Roux, É., Chaouch, M., Diouf, P. N., and Stevanovic, T. (2015). “Impact of a pressurized hot water treatment on the quality of bio-oil produced from aspen,” *Biomass and Bioenergy* 81, 202-209 DOI:10.1016/J.biombioe.2015.07.005
- Lee, M.-K., Tsai, W.-T., Tsaic, Y.-L., and Lin, S.-H. (2010). “Pyrolysis of Napier grass in an induction-heating reactor,” *Journal of Analytical and Applied Pyrolysis* 88(2), 110-116. DOI:10.1016/j.jaap.2010.03.003
- Leibbrandt, N. H., Knoetze, J. H., and Gorgens, J. F. (2011). “Comparing biological and thermochemical processing of sugarcane bagasse: An energy balance perspective,” *Biomass and Bioenergy* 35(5), 2117-2126. DOI:10.1016/j.biombioe.2011.02.017
- Liew, W. H., Hassim, M. H., and Ng, D. K. S. (2014). “Review of evolution, technology and sustainability assessments of biofuel production,” *Journal of Cleaner Production* DOI: 10.1016/j.jclepro.2014.01.006
- Lupoi, J. S., Singh, S., Simmons, B. A., and Henry, R. J. (2014). “Assessment of lignocellulosic biomass using analytical spectroscopy: an evolution to high-throughput techniques,” *BioEnergy Research* 7(1), 1-23. DOI:10.1007/s12155-013-9352-1
- Margeot, A., Hahn-Hagerdal, B., Edlund, M., Slade, R., and Monot, F. (2009). “New improvements for lignocellulosic ethanol,” *Curr. Opin. Biotechnol.* 20(3), 372-380. DOI:10.1016/j.copbio.2009.05.009
- Medvedev, D., Murashkina, A., Pikalova, E., Demin, A., Podias, A., and Tsiakaras, P. (2014). “BaCeO<sub>3</sub>: Materials development, properties and application,” *Progress in Materials Science* 60, 72-129. DOI: 10.1016/j.pmatsci.2013.08.001

- Mimmo, T., Panzacchi, P., Baratieri, M., Davies, C. A., and Tonon, G. (2014). "Effect of pyrolysis temperature on *Miscanthus (Miscanthus x giganteus)* biochar physical, chemical and functional properties," *Biomass and Bioenergy* 62, 149-157. DOI:10.1016/j.biombioe.2014.01.004
- Ming, Z., Ximei, L., Yulong, L., and Lilin, P. (2014). "Review of renewable energy investment and financing in China: Status, mode, issues and countermeasures," *Renewable and Sustainable Energy Reviews* 31, 23-37. DOI:10.1016/j.rser.2013.11.026
- Mohammed, I. Y., Kazi, F. K., Abakr, Y. A., Yusuf, S., and Razzaque, M. A. (2015a). "Novel method for the determination of water content and higher heating value of pyrolysis oil," *BioResources* 10(2), 2681-2690. DOI:10.15376/biores.10.2.2681-2690
- Mohammed, I. Y., Abakr, Y. A., Kazi, F. K., Yusup, S., Alshareef, I., and Chin, S. A. (2015b). "Comprehensive characterization of napier grass as a feedstock for thermochemical conversion," *Energies* 8(5), 3403-3417. DOI:10.3390/en8053403
- Mohammed, I. Y., Abakr, Y. A., Kabir, F., & Yusuf, S. (2015c). "Effect of aqueous pretreatment on pyrolysis characteristics of napier grass. *Journal of Engineering Science & Technology*," 10(11), in press
- Mohammed, I. Y., Samah, M., Mohamed, A., & Sabina, G. (2014). "Comparison of Selexol<sup>TM</sup> and Rectisol<sup>®</sup> Technologies in an Integrated Gasification Combined Cycle (IGCC) Plant for Clean Energy Production," *International Journal of Engineering Research* 3(12), 742-744. <http://works.bepress.com/irpindia/198>
- Mukome, F. N. D., Zhang, X., Silva, L. C. R., Six, J., and Parikh, S. J. (2013). "Use of chemical and physical characteristics to investigate trends in biochar feedstocks," *Journal of Agricultural and Food Chemistry* 61(9), 2196-2204. DOI:10.1021/jf3049142
- Muradov, N., Fidalgo, B., Gujar, A. C., Garceau, N., and T-Raissi, A. (2012). "Production and characterization of *Lemna minor* bio-char and its catalytic application for biogas reforming," *Biomass Bioenergy* 42, 123-131. DOI:10.1016/j.biombioe.2012.03.003
- Nigam, P. S., and Singh, A. (2011). "Production of liquid biofuels from renewable resources," *Prog. Energy Combust Sci.* 37(1), 52-68. DOI:10.1016/j.pecs.2010.01.003
- Oasmaa, A., Leppamaki, E., Koponen, P., Levander, J., and Tapola, E. (1997). "Physical characterization of biomass-based pyrolysis liquids, application of standard fuel oil analyses," *Fuels and Energy Abstracts* 39(2), 97. DOI:10.1016/s0140-6701(98)97220-4
- Oil Market Report (OMR). (2015). International Energy Agency, <https://www.iea.org/oilmarketreport/omrpublic/>
- Oja, V., Hajaligol, M. R., and Waymack, B. E. (2006). "The vaporization of semi-volatile compounds during tobacco pyrolysis," *J. Anal. Appl. Pyrol.* 76(1-2), 117-123. DOI:10.1016/j.jaap.2005.08.005
- Organization of Petroleum Exporting Countries (OPEC). (2013). "Annual Statistical Bulletin," ([http://www.opec.org/opec\\_web/en/data\\_graphs/330.htm](http://www.opec.org/opec_web/en/data_graphs/330.htm)).
- Park, S. R., Pandey, A. K., Tyagi, V. V., and Tyagi, S. K. (2014). "Energy and exergy analysis of typical renewable energy systems," *Renewable and Sustainable Energy Reviews* 30, 105-123. DOI:10.1016/j.rser.2013.09.011
- Phan, B. M. Q., Duong, L. T., Nguyen, V. D., Tran, T. B., Nguyen, M. H. H., Nguyen, L.

- H., Nguyen, D. A., and Luu, L. C. (2014). "Evaluation of the production potential of bio-oil from Vietnamese biomass resources by fast pyrolysis" *Biomass and Bioenergy* 62, 74-81. DOI.org/10.1016/j.biombioe.2014.01.012
- Pilon, G., and Lavoie, J-M. (2011). "Characterization of switchgrass char produced in torrefaction and pyrolysis conditions," *BioResources* 6(4), 4824-4839
- Pütün, E. (2010). "Catalytic pyrolysis of biomass: Effects of pyrolysis temperature, sweeping gas flow rate and MgO catalyst," *Energy* 35(7), 2761-2766. DOI:10.1016/j.energy.2010.02.024
- Raveendran, R., Ganesh, A., and Khilar, K. C. (1996). "Pyrolysis characteristics of biomass and biomass components." *Fuel* 75(8), 987-998. DOI:10.1016/0016-2361(96)00030-0
- Saidura, R., Abdelaziza, E. A., Demirbasb, A., Hossaina, M. S., and Mekhilef, S. (2011). "A review on biomass as a fuel for boilers," *Renewable and Sustainable Energy Reviews* 15(5), 2262-2289. DOI:10.1016/j.rser.2011.02.015
- Samson, R., Mani, S., Boddey, R., Sokhansanj, S., Quesada, D., Urquiaga, S., Reis, V. and Ho Lem, C. (2005). "The potential of C4 perennial grasses for developing a global BIOHEAT industry," *Critical Reviews in Plant Sciences* 24(5-6), 461-495. DOI:10.1080/07352680500316508
- Shihadeh, A., and Hochgreb, S. (2002). "Impact of biomass pyrolysis oil process conditions on ignition delay in compression ignition engines," *Energy & Fuels* 16(3), 552-561. DOI:1/ef010094d
- Sluiter, A., Hames, B., Ruiz, R., Scarlata, C., Sluiter, J., Templeton, D., and Crocker, D. (2012). "Determination of structural carbohydrates and lignin in biomass laboratory analytical procedure," National Renewable Laboratory, NREL/TP-510-42618.
- Soetardji, J. P., Widjaja, C., Djojarahardjo, Y., Soetaredjo, F. E., Ismadjia, S. (2014). "Bio-oil from jackfruit peel waste," *Procedia Chemistry* 9, 158 – 164. DOI:10.1016/j.proche.2014.05.019
- Song, W., and Guo, M. (2012). "Quality variations of poultry litter biochar generated at different pyrolysis temperatures," *J. Anal. Appl. Pyrolysis* 94, 138-145. DOI:10.1016/j.jaap.2011.11.018
- Srirangan, K., Akawi, L., Moo-Young, M., and Chou, C.P. (2012). "Towards sustainable production of clean energy carriers from biomass resources," *Applied Energy* 100, 172-186. DOI:10.1016/j.apenergy.2012.05.012
- Stephanidis, S., Nitsos, C., Kalogiannis, K., Iliopoulou, E. F., Lappas, A. A., and Triantafyllidis, K. S. (2011). "Catalytic upgrading of lignocellulosic biomass pyrolysis vapours: Effect of hydrothermal pre-treatment of biomass," *Catalysis Today* 167, 37-45 DOI:10.1016/j.cattod.2010.12.049
- Strezov, V., Evans, T. J., and Hayman, C. (2008). "Thermal conversion of elephant grass (*Pennisetum purpureum* Schum.) to bio-gas, bio-oil and charcoal," *Bioresource Technology* 99(17), 8394-8399. DOI:10.1016/j.biortech.2008.02.039
- Sun, Y., Gao, B., Yao, Y., Fang, J., Zhang, M., Zhou, Y., Chen, H., and Yang, L. (2014). "Effects of feedstock type, production method, and pyrolysis temperature on biochar and hydrochar properties," *Chemical Engineering Journal* 240, 574-578. DOI:10.1016/j.cej.2013.10.081
- Uzun, B. B., Pütün, A. E., and Pütün, E. (2007). "Rapid pyrolysis of olive residue. 1. Effect of heat and mass transfer limitations on product yields and bio-oil compositions," *Energy & Fuel* 21(3), 1768-1776. DOI:10.1021/ef060171a
- Venderbosch, R. H., and Prins, W. (2010). "Fast pyrolysis technology development –

- Review,” *Biofuels, Bioprod. Biorefin.* 4(2), 178-208. DOI:10.1002/bbb.205
- Wang, D., Zhang, W., Hao, X., and Zhou, D. (2013). “Transport of biochar particles in saturated granular media: Effects of pyrolysis temperature and particle size,” *Environ. Sci. Technol.* 47(2), 821-828. DOI:10.1021/es303794d
- Wang, H., Srinivasan, R., Yu, F., Steele, P., Li, Q., and Mitchell, B. (2011). “Effect of acid, alkali, and steam explosion pretreatments on characteristics of bio-oil produced from pinewood,” *Energy Fuels* 25, 3758-3764. DOI: 10.1021/ef2004909
- Xiu, S., and Shahbazi, A. (2012). “Bio-oil production and upgrading research: A review,” *Renewable and Sustainable Energy Reviews* 16(7), 4406-4414. DOI:10.1016/j.rser.2012.04.028
- Yamamoto, T., Tayakout-Fayolle, M., Geantet, C. (2015). “Gas-phase removal of hydrogen sulfide using iron oxyhydroxide at low temperature: Measurement of breakthrough curve and modeling of sulfidation mechanism”, *Chemical Engineering Journal* 262, 702–709. DOI.org/10.1016/j.cej.2014.09.093
- Yang, H., Yan, R., Chen, H., Lee, D. H., and Zheng, C. (2007). “Characteristics of hemicellulose, cellulose and lignin pyrolysis,” *Fuel Volume* 86(12-13), 1781-1788. DOI:10.1016/j.fuel.2006.12.013
- Yuan, J.-H., Xu, R.-K., and Zhang, H. (2011). “The forms of alkalis in the biochar produced from crop residues at different temperatures,” *Bioresource Technology* 102(3), 3488-3497. DOI:10.1016/j.biortech.2010.11.018
- Zhang, Q., Chang, J., Wang T., and Xu, Y. (2007). “Review of biomass pyrolysis oil properties and upgrading research,” *Energy Conversion and Management* 48(1), 87-92. DOI:10.1016/j.enconman.2006.05.010

Article submitted: April 27, 2015; Peer review completed: July 24, 2015; Revised version received: July 30, 2015; Accepted: July 31, 2015; Published: August 12, 2015.  
DOI: 10.15376/biores.10.4.6457-6478